Uniform Gold Nanorod Arrays from Polyethylenimine-Coated Alumina Templates

Jeong-Mi Moon and Alexander Wei*

Department of Chemistry, 560 Oval Drive, Purdue University, West Lafayette, Indiana 47907-2084

Received: August 7, 2005; In Final Form: September 26, 2005

Monolithic Au nanorod arrays can be grown by electrodeposition in Au-backed nanoporous alumina templates using polyethylenimine (PEI) as an adhesion layer, with excellent height control between 300 nm and 1.4 μm. The local height distribution can be extremely narrow with relative standard deviations well below 2%. The uniform growth rate appears to be determined by the adsorbed PEI matrix, which controls the growth kinetics of the grains comprising the nanorods. The nanorods can be retained as free-standing 2D arrays after careful removal of the AAO template. Reflectance spectroscopy reveals a collective plasmon mode with a maximum near 1.2 μm, in accord with recent calculations for 2D arrays of closely spaced cylindrical nanoparticles.

Introduction

Noble metal nanostructures are well-known to exhibit strong optical extinctions at visible to near-infrared (NIR) wavelengths due to the collective excitation of their conduction electrons, an electrodynamic phenomenon commonly referred to as a surface plasmon.[1,2] Periodic arrays of plasmon-resonant nanomaterials are candidates for photonic devices such as tunable photonic band gaps[3,4] and near-field optical waveguides,[5−7] based on the strong electromagnetic coupling between array elements. This coupling can also generate intense but highly localized electromagnetic fields, which is desirable for enhancing a variety of nonlinear optical effects and spectroscopic sensing modalities such as surface-enhanced Raman scattering (SERS).[8−10] Theoretical studies of metal nanoparticle arrays have indicated that both local and surface-averaged field enhancements can be optimized at a given frequency as a function of size and interparticle spacing.[11−14] We have determined that 2D arrays of closely spaced cylindrical nanoparticles (i.e., nanorods) provide a nearly ideal geometry for generating local field factors with maximum intensity.[14] With respect to size, plasmonic responses scale roughly with particle volume but are limited by size-dependent retardation and damping effects, so the optimal enhancements are most likely produced by arrays of nanorods having diameters between 40 and 100 nm, depending on the wavelength of interest.[1,2,14]

Designing plasmon-resonant nanorod arrays for photonic applications requires a suitable fabrication method, one which enables control over particle size, aspect ratio, and interparticle spacing. Top-down methods such as electron-beam lithography impart excellent spatial control, but at present these are limited in sample throughput and cannot easily provide particle separations of less than 25 nm. Self-assembly methods have been effective for organizing colloidal Au nanospheres[15−19] and nanorods[9,20−24] into close-packed 2D and 3D arrays. However, organizing anisotropic particles such as nanorods into axially oriented, smectic monolayers is much more challenging, with respect to both 2D order and interparticle spacing.

Nanoporous anodized aluminum oxide (AAO) films offers a direct route to metal nanorod arrays with hexagonal 2D order. The electrochemical synthesis of metal nanowires in nanoporous anodized aluminum oxide (AAO) membranes is an established methodology[25,26] and is being widely used to produce individual nanowires as components in nanoscale electronics and photonics.[27−29] Several earlier studies have shown that Au nanorods with controlled aspect ratios can be prepared within AAO membranes primed with Ag.[30−34] Nanoporous AAO films should thus be ideal templates for preparing Au nanorod arrays with uniform height and 2D smectic order, but to the best of our knowledge this subject has not been adequately addressed, aside from some interesting examples of amphiphilic metal−polymer nanorods assembling into micelle-like monolayers.[35] The paucity of work in this area may be related to the challenges of establishing homogeneous growth conditions within each nanopore, which can be perturbed by poor or variable ohmic contact with the cathode.

We set out to fabricate monolithic nanorod arrays within AAO templates by using a thin Au film as the cathode to ensure preparation of a homogeneous material. However, Au has poor adhesion properties and delaminates easily from the nanoporous AAO membrane, necessitating an intermediate layer for bonding. In our experience, direct evaporation of Au onto freshly prepared nanoporous Al_2O_3 substrates resulted in a fail rate of over 90%. Adhesive metals such as Cr are commonly employed, but this can introduce intermetallic diffusion which compromises the dielectric function of the Au nanorods. We thus sought a nonmetallic adhesion layer to enable Au bonding and subsequent electrodeposition.

Here we describe the fabrication of 2D arrays of Au nanorods using nanoporous AAO templates coated with polyethylenimine (PEI), with very fine control over nanorod height. PEI is a branched polyamine well-known for its physisorption properties and can mediate the bonding of nanostructured metals onto planar or curved substrates.[36−41] Low molecular weight PEI is also a common additive in electroplating solutions and often used as a brightener in the electrodeposition of metal films. The PEI-coated templates not only permitted us to circumvent the issue of metal contamination but also proved to be uniquely suited for growing Au nanorods of uniform size and height.

* Corresponding author: Tel (765) 494-5257; Fax (765) 494-0239; E-mail alexwei@purdue.edu.

10.1021/jp054405n CCC: $30.25
Published on Web 11/17/2005

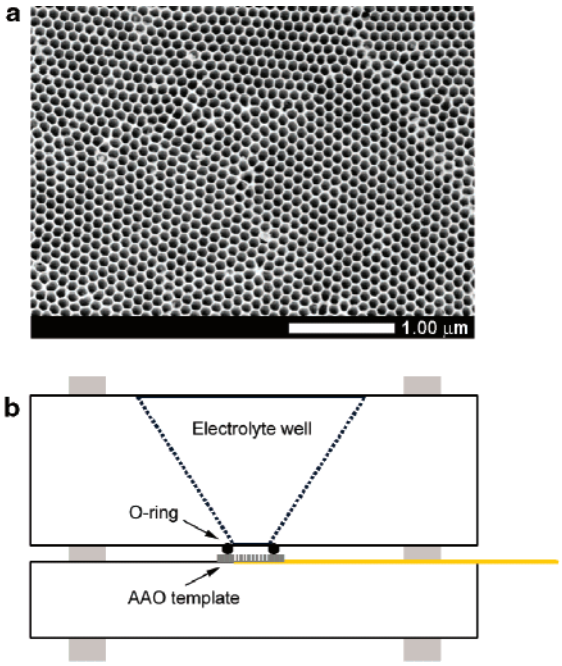

Figure 1. (a) Plan-view FE-SEM image of AAO membrane with 75 nm pores, produced by a two-step anodization process followed by treatment in 0.8% H_3PO_4 at 30 °C. (b) Schematic of electrochemical cell.

Experimental Section

Reagents and Materials Characterization. High-purity Al foil (99.999%, 0.2 in. thickness) was purchased from Research and PVD Materials. Au electroplating solution (Orotemp 24) was obtained from Technic Inc. High molecular weight PEI (MW ~750 000, 50 wt % solution) was purchased from Aldrich and used without further purification. (Aminopropyl)triethoxysilane (APTES) was obtained from Pierce and purified by reduced-pressure distillation. Deionized water was obtained from an ultrafiltration system (Milli-Q, Millipore) with a measured resistivity above 18 MΩ·cm and passed through a 0.22 μm filter to remove particulate matter. All nanostructured materials were characterized using a Hitachi S-4800 field-emission scanning electron microscope (FE-SEM).

Preparation of Nanoporous AAO Template. Al foil was sonicated in trichloroethylene for 1 h and washed with deionized water prior to anodization. The foils were electropolished for 4 min (10 °C, 14 V) in a solution containing 70% perchloric acid (70 mL) and ethanol (350 mL) using a dc power supply (Sorensen DCR 40-20A) and then thoroughly washed with deionized water. Nanoporous AAO templates were prepared by a two-step anodization process.[42,43] Al foil was first anodized in a 0.3 M oxalic acid solution at 5 °C at a constant applied voltage of 40 V for 20 h and then etched in an aqueous mixture of phosphoric acid (6 wt %) and chromic acid (1.8 wt %) at 60 °C. A second anodization was performed for 8−11 h using the same conditions as above, followed by dissolution of the remaining Al in a saturated $HgCl_2$ solution. Pore widening and removal of the barrier oxide layer were carried out by chemical etching in 0.8 wt % phosphoric acid at 30 °C for 60 min to produce AAO films with highly ordered pores (diameter = 75 nm, center-to-center distance = 105 nm; see Figure 1).

Preparation of Adhesion Layer and Au Cathode. Freshly prepared AAO templates were soaked in aqueous PEI solutions (0.05−5 wt %) for 5 h at room temperature. The PEI-coated templates were washed by soaking them six consecutive times in deionized water baths (10 min each) and then dried overnight in a vacuum oven at 70 °C. For modification with APTES, the AAO templates were soaked in a 0.2 M toluene solution at 120 °C for 4 h, washed with toluene several times, and then dried in a vacuum oven. A thin film of Au (~40 nm) was thermally evaporated onto one face of the modified AAO template. FE-SEM revealed an evenly deposited layer of Au on the substrate surface, with a pore penetration depth of less than 50 nm.

Electrosynthesis of Au Nanorod Arrays and Removal of AAO Template. Electrodepositions were conducted using a PAR 273A potentiostat/galvanostat with a Pt wire counter electrode and a saturated calomel electrode (SCE) as a reference. In a typical experiment, a 1 cm^2 Au-backed AAO membrane was attached to a conductive Cu tape and covered by a 7 mm rubber O-ring and then placed in a homemade Teflon electroplating cell with the open pores exposed to the electrolyte well (see Figure 1). Electrodepositions were performed at ambient temperatures under galvanostatic conditions at currents of 485 or 48.5 μA (current densities of 1260 or 126 μA/cm^2, respectively). The AAO template was dissolved using a 2 M KOH solution in 90% ethylene glycol, with gentle agitation at 43 °C for 3 h using an orbital shaker. The immobilized substrate was washed several times with water and ethanol, and the residual solvent was removed using a critical point dryer (SPI-Dry, Structure Probe) with CO_2 as the supercritical medium.

Results and Discussion

Freshly prepared AAO membranes with a mean pore diameter of 75 nm were immersed in 0.05%, 0.5%, or 5% PEI solutions, thoroughly washed in deionized water, and then dried in a vacuum oven overnight. The PEI was determined to be well dispersed prior to adsorption onto the AAO surface, with an average radius of gyration of 38 nm based on dynamic light scattering. Thin Au films (thickness ~40 nm) were then deposited by thermal evaporation and determined to be firmly adhered onto the PEI-treated substrates by visual inspection as well as by FE-SEM.

The Au/PEI/AAO membranes proved to be excellent templates for the uniform electrochemical growth of metal nanorods. Templates soaked in 5% PEI solution prior to Au evaporation produced the best results: uniform 2D arrays of Au nanorods could be fabricated for electrodepositions of 0.5, 1.0, and 2.0 C, with average height H = 0.30, 0.69, and 1.33 μm, respectively (see Figure 2 and Supporting Information). The local standard deviations (SDs) in height within a 1−3 μm sector (σ_{local}) were 0.02, 0.05, and 0.06 μm, respectively; the SDs measured across the entire membrane were nearly identical (σ_{global} = 0.02, 0.07, and 0.06 μm, respectively). These low SD values demonstrate the homogeneity in local growth conditions provided by the PEI-modified AAO templates. The nanorods were linearly proportional to the amount of expended charge up to 2.0 C but became uneven with further electrodeposition, indicating a change in growth conditions beyond a threshold height (see Supporting Information). Nevertheless, the mean height H of the Au nanorods is nearly constant over the entire substrate, with significant deviations only at the edges of the cell window (see Figure 2d). This suggests that PEI-modified alumina templates have the capacity to produce uniform nanorods on an increased lateral scale, an issue of practical relevance for technological considerations.

The height distribution of the nanorods could be further improved by reducing the electrodeposition rate (see Figure 3). Lowering the current density from 1260 to 126 μA/cm^2 produced nanorod arrays with remarkably narrow size dispersities: for a deposition of 2.07 C, H = 1.416 ± 0.024 μm

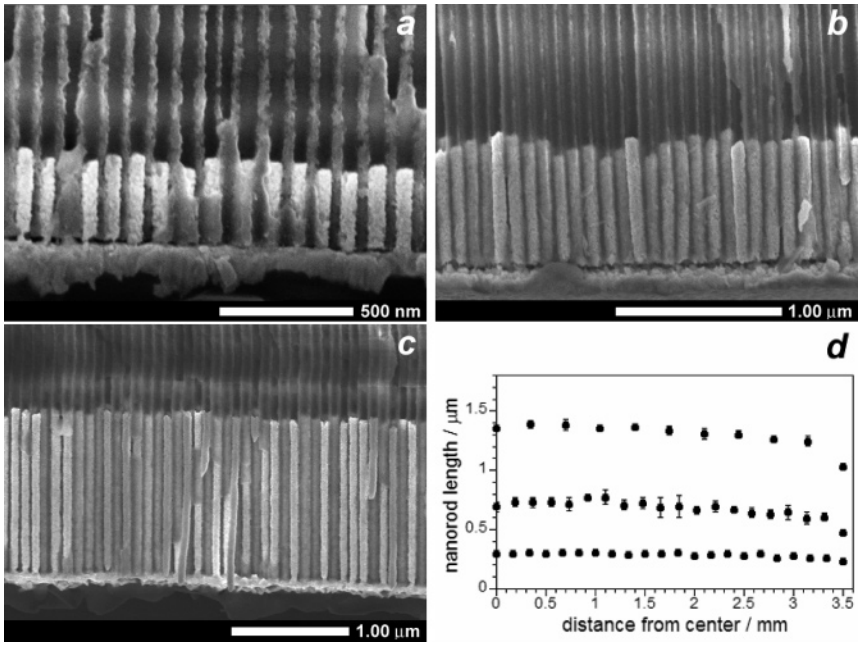

Figure 2. FE-SEM images of Au nanorods ($d = 75$ nm) as a function of delivered charge: (a) 0.5 C ($H = 0.30 \pm 0.02$ μm); (b) 1.0 C ($H = 0.69 \pm 0.05$ μm); (c) 2.0 C ($H = 1.33 \pm 0.06$ μm). Nanorods were grown at a current density of 1260 μA/cm^2, using AAO templates coated in a 5% PEI solution. (d) Nanorod heights (in μm) measured as a function of distance from the center of the template (in mm).

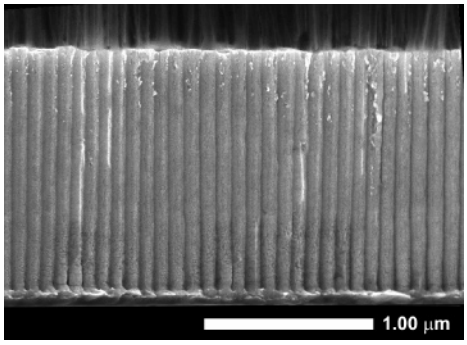

Figure 3. FE-SEM image of 1.396 ± 0.007 μm Au nanorods, produced in AAO templates coated in a 5% PEI solution (2.07 C, 126 μA/cm^2).

(relative SD = 1.7%) with σ_{local} as low as 0.007 μm (relative SD = 0.5%). The beneficial effect of reduced current density is most likely due to the suppression of kinetically driven growth processes, although it must be mentioned that the amount of adsorbed PEI is also important for uniform nanorod growth (see below).

To evaluate the quality of the nanorod array in two dimensions, the AAO template was removed by exposure to KOH under mild conditions, followed by several washes with water and ethanol. The residual solvent was removed with minimal disturbance to the nanorods by coevaporation with supercritical CO_2 using a critical point dryer. Plan-view images of the free-standing nanorod arrays confirmed an essentially quantitative fill ratio, with a few sites having lower backscatter contrast (see Figure 4). A closer inspection of these sites revealed that nearly all of them are occupied by slightly shorter nanorods, in accord with the cross-sectional images in Figure 2.

AAO substrates coated in diluted PEI solutions also produced Au nanorod arrays with uniform mean heights across the substrate, albeit with broader height distributions. Electrodepositions in Au/PEI/AAO membranes prepared from 0.5% and 0.05% PEI solutions were performed using similar conditions as the 5% PEI case (2.0 C, 1260 μA/cm^2) to produce nanorods with comparable mean heights but larger SDs ($H = 1.62 \pm 0.22$ and 1.59 ± 0.18 μm, respectively; see Supporting Information for details). Reducing the current density by 10-fold (2.0 C, 126 μA/cm^2) again resulted in narrower height distributions; in the case of 0.5% PEI, the mean height was determined to be $H = 1.38 \pm 0.06$ μm, nearly identical to the 5% PEI case at the higher current density (cf. Figure 2c).

The homogeneity of the nanorod growth conditions provided by the PEI-modified templates is remarkable when compared with electrodepositions performed in unmodified AAO templates or in templates coated with 3-aminopropyltriethoxysilane

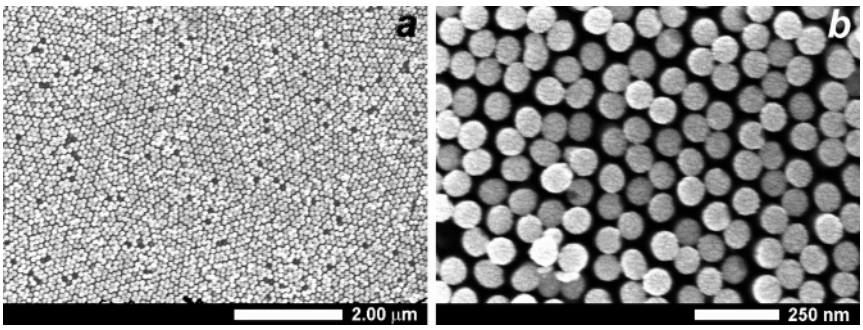

Figure 4. (a) Plan view (×10K magnification) of free-standing Au nanorod array fabricated in AAO templates coated with 5% PEI (1.0 C, 1260 μA/cm^2), followed by template removal and critical point drying. Slightly shorter nanorods have a lower backscatter contrast but are discernible upon close inspection in most cases. (b) Same as above, ×100K magnification.

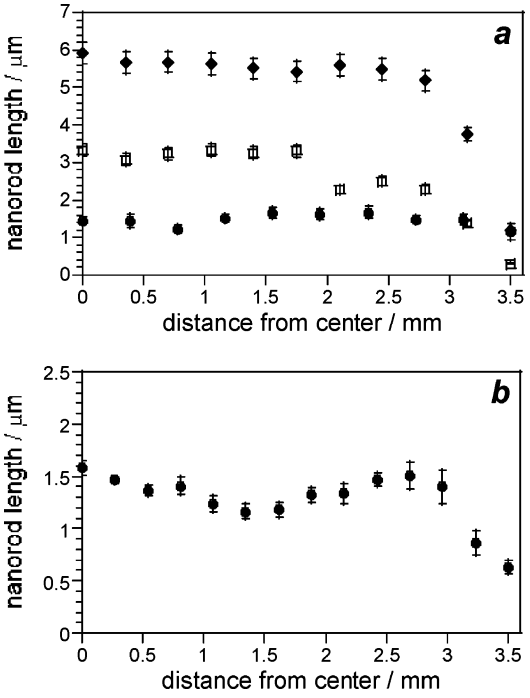

Figure 5. Nanorod heights (in μm) produced in Au-backed AAO templates coated with (a) APTES (0.5 C (circles), 1.0 C (squares), and 2.0 C (diamonds), 1260 μA/cm^2) or (b) without organic coatings (0.78 C, 1260 μA/cm^2), measured as a function of distance from the center of the AAO template (in mm).

(APTES). Two differences are immediately apparent with the latter substrates: (i) the local nanorod heights are less even with respect to their position within the substrate, and (ii) the overall heights are considerably greater than those produced in the PEI-coated substrates under identical electrodeposition conditions (see Figure 5). The reasons for the uneven height distributions are not entirely clear, but one possibility is that the relatively poor adhesion of Au on these AAO membranes renders the cathodic interface suspectible to sample stress, resulting in a substantial increase in contact resistance near the edge of the cell.

The fine degree of control in nanorod height provided by the PEI-coated AAO templates is offset by a reduction in plating efficiency H/H_0, with the theoretical nanorod height calculated as $H_0 = Q/nFAV_m$, where Q is the total charge, n is the number of electrons in the plating reaction, F is Faraday's constant, A is the total area of exposed pores, and V_m is the molar volume defined as specific gravity divided by formula weight, which for Au is 0.099.[44] This yields $H_0 = 4.86$ μm/C, corresponding to an efficiency of ~14%. In comparison, the typical plating efficiency in metal-backed AAO templates without a PEI adhesion layer is 70%.[45] The lower efficiency can be related to several factors: (i) reduced ion mobility through the PEI matrix, (ii) a more negative potential (i.e., a higher overpotential) for the reduction of Au(I)−polyamine complexes, and (iii) a less negative potential for hydrogen production catalyzed by the polyamine coating, via the reduction of their conjugate acids after an initial proton transfer (eq 1):[46]

$$RR'NH_2^+ + e^- \rightarrow RR'NH + {}^1/_2H_2 \qquad (1)$$

High-magnification FE-SEM images of the Au nanorods within the PEI-coated AAO templates reveals a grain size on the order of 10−15 nm (see Figure 6). Surface asperities of comparable dimensions are also evident near the base of the nanorods, where the PEI density should be greatest. The small grain size is consistent with a nucleation−coalescence growth mechanism,[47] which is favored by the high overpotential of the Au−polyamine system. Nucleation−coalescence is typically the dominant mechanism during metal electrodeposition, and careful optimization of growth conditions is necessary for the electrosynthesis of single-crystal nanorods and nanowires.[48]

These observations suggest that the PEI adsorbed on the nanopore walls is highly effective at suppressing crystalline growth kinetics by passivating the grains' surfaces. Similar growth-limiting effects by polyamines have been observed in the chemical synthesis of metal nanoparticles within polymer films and dendrimers.[49−52] Surface passivation in conjunction with a reduced current density (see above) ensures that grain coalescence is the rate-determining step in the slow but uniform growth of gold nanorods. However, as the diffusion of high MW PEI into the AAO channels can be expected to have a finite penetration depth, kinetic growth processes should increase in significance if the electrodeposition extends beyond the PEI-coated region, with a subsequent loss of control in nanorod height (see Supporting Information). Increasing the penetration depth of PEI adsorption into the AAO channels may further extend the fine control over nanorod growth to several microns in length.

The free-standing monolithic Au nanorod array in Figure 4 (mounted on a glass coverslip) produces two strong NIR responses as measured by reflectance−absorbance spectroscopy, near 1.22 μm and beyond 2 μm (see Figure 7). Control measurements of glass and Au-backed alumina confirmed the high levels of transmittance and reflectance, respectively, of these substrates at NIR wavelengths, which implies that the optical response from the nanorod array arises essentially from resonant backscattering. The NIR resonance at 1.22 μm can be ascribed to strongly coupled transverse plasmon modes between closely spaced nanorods, in accord with theoretical studies on the electromagnetic field factors produced by 2D arrays of cylindrical metal nanoparticles.[14] The longitudinal plasmon modes of the nanorods are not expected to contribute to this resonance but may be responsible for the scattering response beyond 2 μm, commensurate with theoretical and experimental

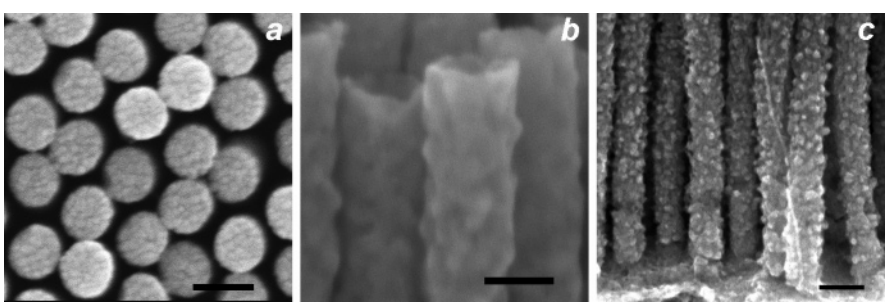

Figure 6. (a) FE-SEM image revealing grain boundaries at nanorod tips; (b) surface structure near nanorod tips; (c) surface asperities near the cathode base. Scale bar = 100 nm.

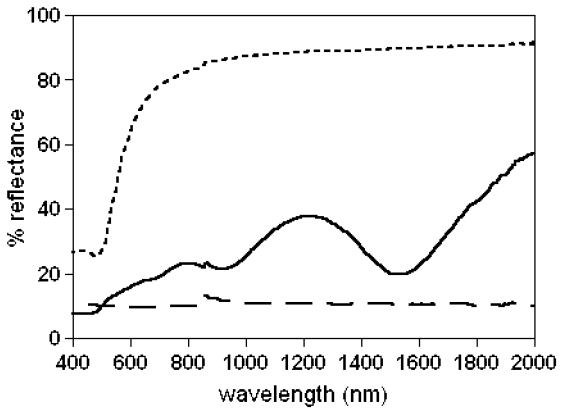

Figure 7. Visible−NIR optical reflectance spectra of monolithic Au nanorod array (cf. Figure 4) and control samples: free-standing nanorod array mounted on glass coverslip using nail polish (solid line); Au-backed AAO template (unfilled) treated with PEI (short dash); glass coated with nail polish and PEI (long dash). Spectra were acquired using a Perkin-Elmer Lambda 950 photospectrometer in back-reflection mode.

studies on Au nanorods with aspect ratios on the order of 20.[34,53] It is worth mentioning that the line width of the collective plasmon resonance at 1.22 μm, while broad (fwhm $\sim$ 350 nm), is substantially narrower than that produced by close-packed 2D arrays of colloidal gold nanoparticles.[8,15] The quality factor should be further improved by increasing the long-range order of the nanorod arrays, such that the spacings between nanorod elements are well-defined.

Conclusion

Polyethylenimine-coated AAO membranes provide significant benefits for the templated synthesis of Au nanorods: the PEI serves as a nonmetallic adhesion layer for the thermal deposition of Au and controls grain size and growth rate during the electrodeposition process. The latter is important for producing Au nanorods with identical aspect ratios, with heights of 1.4 μm and σ_{local} and σ_{global} values of 0.007 and 0.024 μm (relative SDs of 0.5% and 1.7%, respectively) having been achieved in our laboratory. The uniformity of the electrosynthesized nanorods depends on the controlled growth and monodispersity of their constituent grains, mediated by the PEI matrix. The nanorods can be retained as monolithic, free-standing 2D arrays and exhibit specific NIR resonances as a function of their collective transverse plasmon modes.

Acknowledgment. The authors gratefully acknowledge financial support from the National Science Foundation (CHE-0243496, ECS-0210445), the National Institutes of Health (EB-001777-01), and the Defense Advanced Research Projects Agency (MDA972-03-0020) in association with the Birck Nanotechnology Center. FE-SEM images were taken at the Purdue Materials Science and Engineering Microscopy Facility. We also thank Alexander Ribbe for his kind assistance with metal evaporation, Vladimir Shalaev and Vladimir Drachev for the use of their optical reflectometer, Rashid Bashir and Amit Gupta for the use of their critical point dryer, Sungho Park for the design of the electrochemical cell, and Kyoung-Shin Choi, Tim Sands, and Manuel DaSilva for helpful discussions.

Supporting Information Available: Size distribution histograms and additional FE-SEM images of Au nanorod arrays produced under nonuniform growth conditions. This material is available free of charge via the Internet at http://pubs.acs.org.

References and Notes

(1) Kreibig, U.; Vollmer, M. *Optical Properties of Metal Clusters*; Springer: New York, 1995; Vol. 25.
(2) Wei, A. In *Nanoparticles: Scaffolds and Building Blocks*; Rotello, V. M., Ed.; Kluwer Academic: New York, 2004; pp 173−200.
(3) Moroz, A. *Phys. Rev. Lett.* **1999**, *83*, 5274−5277.
(4) Zhang, W. Y.; Lei, X. Y.; Wang, Z. L.; Zheng, D. G.; Tam, W. Y.; Chan, C. T.; Sheng, P. *Phys. Rev. Lett.* **2000**, *84*, 2853−2856.
(5) Maier, S. A.; Kik, P. G.; Atwater, H. A.; Meltzer, S.; Harel, E.; Koel, B. E.; Requicha, A. A. G. *Nat. Mater.* **2003**, *2*, 229−232.
(6) Wurtz, G. A.; Im, J. S.; Gray, S. K.; Wiederrecht, G. P. *J. Phys. Chem. B* **2003**, *107*, 14191−14198.
(7) Paniou, N.-C.; Osgood, R. M., Jr. *Nano Lett.* **2004**, *4*, 2427−2430.
(8) Wei, A.; Kim, B.; Sadtler, B.; Tripp, S. L. *Chem. Phys. Chem.* **2001**, *2*, 743−745.
(9) Tao, A.; Kim, F.; Hess, C.; Goldberger, J.; He, R.; Sun, Y.; Xia, Y.; Yang, P. *Nano Lett.* **2003**, *3*, 1229−1233.
(10) Félidj, N.; Truong, S. L.; Aubard, J.; Lévi, G.; Krenn, J. R.; Hohenau, A.; Leitner, A.; Aussenegg, F. R. *J. Chem. Phys.* **2004**, *120*, 7141−7146.
(11) Wirgin, A.; López-Ríos, T. *Opt. Commun.* **1984**, *48*, 416−420.
(12) Garcia-Vidal, F. J.; Pendry, J. B. *Phys. Rev. Lett.* **1996**, *77*, 1163−1166.
(13) Xu, H.; Aizpurua, J.; Käll, M.; Apell, P. *Phys. Rev. E* **2000**, *62*, 4318−4324.
(14) Genov, D. A.; Sarychev, A. K.; Shalaev, V. M.; Wei, A. *Nano Lett.* **2004**, *4*, 153−158.
(15) Kim, B.; Tripp, S. L.; Wei, A. *J. Am. Chem. Soc.* **2001**, *123*, 7955−7956.
(16) Kim, B.; Carignano, M. A.; Tripp, S. L.; Wei, A. *Langmuir* **2004**, *20*, 9360−9365.
(17) Kim, B.; Balasubramanian, R.; Pérez-Segarra, W.; Wei, A.; Decker, B.; Mattay, J. *Supramol. Chem.* **2005**, *17*, 173−180.
(18) Tessier, P. M.; Velev, O. D.; Kalambur, A. T.; Rabolt, J. F.; Lenhoff, A. M.; Kaler, E. W. *J. Am. Chem. Soc.* **2000**, *122*, 9554−9555.
(19) Graf, C.; van Blaaderen, A. *Langmuir* **2002**, *18*, 524−534.
(20) Nikoobakht, B.; Wang, Z. L.; El-Sayed, M. A. *J. Phys. Chem. B* **2000**, *104*, 8635−8640.
(21) Kim, F.; Kwan, S.; Akana, J.; Yang, P. *J. Am. Chem. Soc.* **2001**, *123*, 4360−4361.
(22) Li, L. S.; Walda, J.; Manna, L.; Alivisatos, A. P. *Nano Lett.* **2002**, *2*, 557−560.
(23) Li, L. S.; Alivisatos, A. P. *Adv. Mater.* **2003**, *15*, 408−410.
(24) Orendorff, C. J.; Hankins, P. L.; Murphy, C. J. *Langmuir* **2005**, *21*, 2022−2026.
(25) Martin, C. R. *Science* **1994**, *266*, 1961−1966.
(26) Nielsch, K.; Müller, F.; Li, A.-P.; Gösele, U. *Adv. Mater.* **2000**, *12*, 582−586.
(27) Dickson, R. M.; Lyon, L. A. *J. Phys. Chem. B* **2000**, *104*, 6095−6098.
(28) Nicewarner-Peña, S. R.; Freeman, R. G.; Reiss, B. D.; He, L.; Peña, D. J.; Walton, I. D.; Cromer, R.; Keating, C. D.; Natan, M. J. *Science* **2001**, *294*, 137−141.
(29) Mbindyo, J. K. N.; Mallouk, T. E.; Mattzela, J. B.; Kratochvilova, I.; Razavi, B.; Jackson, T. N.; Mayer, T. S. *J. Am. Chem. Soc.* **2002**, *124*, 4020−4026.
(30) Foss, C. A., Jr.; Hornyak, G. L.; Stockert, J. A.; Martin, C. R. *J. Phys. Chem.* **1992**, *96*, 7497−7499.
(31) Foss, C. A., Jr.; Hornyak, G. L.; Stockert, J. A.; Martin, C. R. *J. Phys. Chem.* **1994**, *98*, 2963−2971.
(32) Hornyak, G. L.; Patrissi, C. J.; Martin, C. R. *J. Phys. Chem. B* **1997**, *101*, 1548−1555.
(33) Van der Zande, B. M. I.; Pagès, L.; Hikmet, R. A. M.; van Blaaderen, A. *J. Phys. Chem.* **1999**, *103*, 5761−5767.
(34) van der Zande, B.; Böhmer, M. R.; Fokkink, L. G. J.; Schönenberger, C. *Langmuir* **2000**, *16*, 451−458.
(35) Park, S.; Lim, J.-H.; Chung, S.-W.; Mirkin, C. A. *Science* **2004**, *303*, 348−51.
(36) Schmitt, J.; Mächtle, P.; Eck, D.; Möhwald, H.; Helm, C. A. *Langmuir* **1999**, *15*, 3256−3266.
(37) Sun, S.; Anders, S.; Thomson, T.; Baglin, J. E. E.; Toney, M. F.; Hamann, H. F.; Murray, C. B.; Terris, B. D. *J. Phys. Chem. B* **2003**, *107*, 5419−5425.
(38) Bon, P.; Zhitomirsky, I.; Embury, J. D. *Surf. Eng.* **2004**, *20*, 5−10.
(39) Sadtler, B.; Wei, A. *Chem. Commun.* **2002**, 1604−1605.
(40) Wang, L.; Sasaki, T.; Ebina, Y.; Kurashima, K.; Watanabe, M. *Chem. Mater.* **2002**, *14*, 4827−4832.
(41) Zhao, Y.; Sadtler, B.; Min, L.; Hockerman, G. H.; Wei, A. *Chem. Commun.* **2004**, 784−785.
(42) Masuda, H.; Fukuda, K. *Science* **1995**, *268*, 1466−68.
(43) Masuda, H.; Satoh, M. *Jpn. J. Appl. Phys., Part 2* **1996**, *35*, L126.

(44) Wang, J.; Tian, M.; Kurtz, J.; Mallouk, T. E.; Chan, M. H. W. *Nano Lett.* **2004**, *4*, 1313−1318.
(45) Moon, J.-M. Purdue University at West Lafayette, IN, unpublished results.
(46) Gourley, R. N.; Grimshaw, J.; Millar, P. G. *J. Chem. Soc. C* **1970**, 2318−2323.
(47) Paunovic, M.; Schlesinger, M. *Fundamentals of Electrochemical Deposition*; John Wiley and Sons: New York, 1998.
(48) Tian, M.; Wang, J.; Kurtz, J.; Mallouk, T. E.; Chan, M. H. W. *Nano Lett.* **2003**, *3*, 919−923.
(49) Spatz, J. P.; Roescher, A.; Möller, M. *Adv. Mater.* **1996**, *8*, 337−340.
(50) Spatz, J. P.; Herzog, T.; Mossmer, S.; Ziemann, P.; Möller, M. *Adv. Mater.* **1999**, *11*, 149−153.
(51) Kim, M.-K.; Jeon, Y.-M.; Jeon, W. S.; Kim, H.-J.; Hong, S. G.; Park, C. G.; Kim, K. *Chem. Commun.* **2001**, 667−668.
(52) Wang, Y.; Yang, J.; Zheng, Z.; Carducci, M. D.; Jiao, J.; Seraphin, S. *Angew. Chem., Int. Ed.* **2001**, *40*, 549−552.
(53) Jana, N. R.; Gearheart, L.; Murphy, C. J. *J. Phys. Chem. B* **2001**, *105*, 4065−4067.